5782 *Biochemistry* **2009,** *48,* 5782–5784
DOI: 10.1021/bi900781u

BIOCHEMISTRY
including biophysical chemistry & molecular biology
Rapid Report

Significantly Improved Sensitivity of Q-Band PELDOR/DEER Experiments Relative to X-Band Is Observed in Measuring the Intercoil Distance of a Leucine Zipper Motif Peptide (GCN4-LZ)†

Harishchandra Ghimire,‡ Robert M. McCarrick,‡ David E. Budil,§ and Gary A. Lorigan*,‡

‡*Department of Chemistry and Biochemistry, Miami University, Oxford, Ohio 45056, and* §*Department of Chemistry and Chemical Biology, Northeastern University, Boston, Massachusetts 02115*

Received May 6, 2009; Revised Manuscript Received May 28, 2009

ABSTRACT: Pulsed electron double resonance (PELDOR)/double electron−electron resonance (DEER) spectroscopy is a very powerful structural biology tool in which the dipolar coupling between two unpaired electron spins (site-directed nitroxide spin-labels) is measured. These measurements are typically conducted at X-band (9.4 GHz) microwave excitation using the four-pulse DEER sequence and can often require up to 12 h of signal averaging for biological samples (depending on the spin-label concentration). In this work, we present for the first time a substantial increase in DEER sensitivity obtained by collecting DEER spectra at Q-band (34 GHz), when compared to X-band. The huge boost in sensitivity (factor of 13) demonstrated at Q-band represents a 169-fold decrease in data collection time, reveals a greatly improved frequency spectrum and higher-quality distance data, and significantly increases sample throughput. Thus, the availability of Q-band DEER spectroscopy should have a major impact on structural biology studies using site-directed spin labeling EPR techniques.

Pulsed electron double resonance (PELDOR)/double electron−electron resonance (DEER) spectroscopy is a rapidly emerging, powerful structural biology technique in which the dipolar coupling between two unpaired electron spins (usually site-directed nitroxide spin-labels) is measured (*1*−*3*). The strength of the dipolar coupling can then be used to determine the distance between the two spins in the range of 2−8 nm (*4*−*9*). This allows researchers to gain valuable structural information from samples in which other techniques like solution NMR or X-ray crystallography prove difficult or impossible (*10*−*12*). These measurements are typically conducted with X-band (9.4 GHz) microwave excitation using the four-pulse DEER sequence and can often require up to 12 h of signal averaging (depending upon concentration) for typical biological samples. In this work, we report for the first time a substantial increase in sensitivity that is obtained by collecting DEER spectra using a pulse Q-band (34 GHz) EPR spectrometer. The huge boost in sensitivity at Q-band reveals higher-quality data and significantly reduces data acquisition time.

For this study, an α-helical coiled coil peptide with a leucine zipper (LZ) motif (residues 245−281) of yeast transcriptional activator GCN4 (*13*, *14*) (Protein Data Bank entry 1YSA) was used as a model. The peptide was synthesized on a solid-state peptide synthesizer with a single TOAC nitroxide spin-label at position 248 with Gln → TOAC substitution for the distance measurements between the two monomers. The TOAC (*15*−*19*) spin-label was chosen over the traditional MTSL (*1*, *14*) to eliminate disproportionation of the two label disulfide bonds to form a linked peptide dimer, and to avoid the motional flexibility of the MTSL nitroxide group for more accurate intercoil backbone distance measurements. In previously published results, the distance between two spin-labels as determined via DEER studies matches the predicted distance from the X-ray crystal structure (*13*, *20*).

Samples for DEER measurements were prepared at a concentration of 200 μM peptide in phosphate buffer consisting of 40 mM potassium phosphate, 50 mM NaCl, and 30% sucrose which was added as a cryoprotectant, at pH 7.0. The data were collected at the Ohio Advanced EPR Laboratory using the newly installed Bruker ELEXSYS E580 spectrometer equipped with a SuperQ-FT pulse Q-band system and EN5107D2 resonator. The electron spin echo-detected EPR spectrum of the doubly labeled GCN4 peptide is shown in Figure 1. The high signal-to-noise ratio was achieved in a single scan with 200 averaged echoes per data point (100 each with a two-step phase cycling).

Figure 2 shows the DEER data sets collected with 10, 100, and 1000 scans at both X- and Q-bands scaled for noise level comparisons. It is immediately obvious that the data collected at Q-band show a much higher signal-to-noise ratio. The signal enhancement at Q-band was measured to be approximately 13-fold. The boost in signal-to-noise is quite remarkable considering the greatly reduced sample volumes used in the Q-band experiments (5 μL vs 20 μL for X-band). We have observed comparable signal-to-noise ratio enhancements on MTSL proteins at Q-band experiments (data not shown). The enhanced sensitivity observed at Q-band stems from a increase in the Boltzmann population difference between the spin states at the higher Zeeman energy, which contributes a factor of ∼4, and

†This work is supported by NIGMS/NIH Grant GM60259-01, Army CDMRP Grant W81XWH-06-1-0551, and NSF Grants CHE-0645709 and MRI-0722403.

*To whom correspondence should be addressed. E-mail: garylorigan@muohio.edu. Telephone: (513) 529-3338. Fax: (513) 529-5715.

 Published on Web 05/28/2009

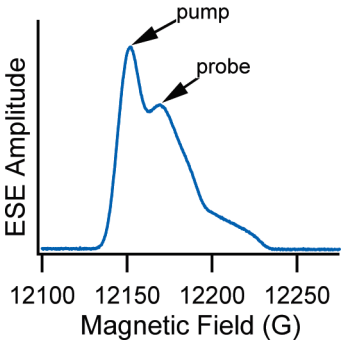

FIGURE 1: Electron spin echo-detected EPR spectrum of the GCN4 peptide at Q-band. Instrument conditions: microwave frequency, 34.186 GHz; pulse widths, 16/32 ns; τ, 200 ns; shot repetition time, 500 μs; number of echoes per point, 100; phase cycling, two-step; number of scans, one; temperature, 80 K.

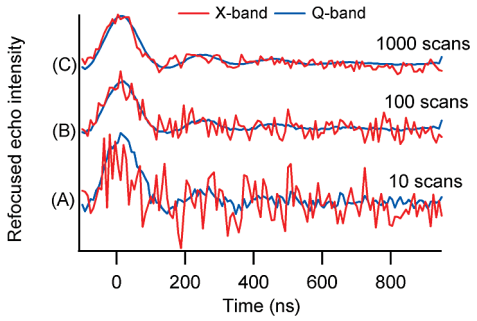

FIGURE 2: DEER comparison of the signal-to-noise ratio of the refocused echo intensity at X-band (red traces) and Q-band (blue traces) for (A) 10 scans (2 min, 40 s), (B) 100 scans (27 min), and (C) 1000 scans (4 h, 27 min). X-Band instrument conditions: probe frequency, 9.265 GHz; pump frequency, 9.200 GHz; probe pulse width, 16/32 ns; pump pulse width, 36 ns; τ, 200 ns; shot repetition time, 500 μs; number of echoes per point, 100; phase cycling, two-step; temperature, 80 K. Q-Band instrument conditions: probe frequency, 34.186 GHz; pump frequency, 34.248 GHz; probe pulse width, 20/40 ns; pump pulse width, 44 ns; τ, 200 ns; shot repetition time, 500 μs; number of echoes per point, 100; phase cycling, two-step; temperature, 80 K.

an increased sensitivity of the instrument/resonator at the higher frequency (*21*, *22*) (P. Hofer, personal communication).

Figure 3 shows Pake patterns in the frequency domain and the corresponding distance distributions obtained at X-band (Figure 3A,B) and Q-band (Figure 3C,D). The increased sensitivity in the time domain translates directly into an improvement in the frequency spectrum and a more accurate distance distribution plot. The spectra were analyzed using Matlab and the DeerAnalysis2008 package provided by the Jeschke laboratory (*23*, *24*). For the Q-band data, the complete Pake pattern is very well resolved; in addition, small inflections corresponding to different subpopulations of the distance distribution are clearly resolved above the noise level. The main peak in the Q-band distance distribution is better resolved (full width at half-height, 1.85 nm), yielding a distance of 2.32 nm. In contrast, a relatively broader peak (full width at half-height, 2.55 nm) corresponding to a distance of 2.27 nm is observed at X-band.

The improved sensitivity observed at Q-band will enable low-frequency components to be more easily detected out of the noise level. Thus, DEER data can be collected for longer pulse delay times, enabling measurement of weaker dipolar couplings (longer distances), resulting in better L curves for more accurate distance measurements.

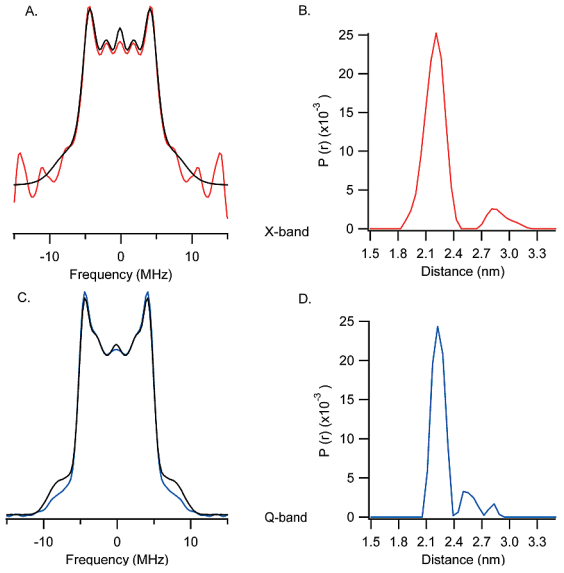

FIGURE 3: Frequency domain and distance distribution at X-band (A and B) and Q-band (C and D). X-Band: zero time, 108 ns; phase, 30.4; background, 263 ns; regularization parameter, 1; distance, 2.27 nm. Q-Band: zero time, 115 ns; phase, 4.7; background, 348 ns; regularization parameter, 0.001; distance, 2.32 nm. The simulations are colored black.

Over the past few years, one of the biggest technological breakthroughs in solution NMR spectroscopy and structural biology has been the development of the cryoprobe technology, which increases the signal-to-noise ratio in NMR spectra by 3−4 depending on the salt content (*25*). This has significantly increased the productivity in solution NMR laboratories by reducing the signal acquisition time and increased sample throughput by 9−16-fold. In a much more dramatic fashion, the 13-fold boost in sensitivity for the Q-band DEER measurements shown in this work theoretically represents a 169-fold decrease in data acquisition time. It is apparent from Figure 2 that the data collected with 1000 scans at X-band are comparable to the data collected with only 10 scans at Q-band. Thus, research laboratories conducting DEER experiments at Q-band will be able to analyze multiple biological samples in a single day, which will dramatically improve productivity. The remarkable boost in sensitivity at Q-band will also enable researchers to conduct experiments at much smaller, more biologically relevant sample concentrations.

In conclusion, we have clearly demonstrated a significant boost in the sensitivity of DEER spectroscopy at Q-band when compared to X-band. Considering the overall improvement in the signal-to-noise ratio, the sample volume requirement (≈4−5 μL at Q-band vs ≈20 μL at X-band), the signal averaging time, and the ease of data analysis, conducting DEER experiments at Q-band is much more advantageous for measuring spin-label−spin-label distances in proteins and peptides than the X-band counterpart. The availability of Q-band DEER can thus be expected to have a major impact on structural biology studies based on site-directed spin labeling.

ACKNOWLEDGMENT

We thank Ralph Weber and Peter Hofer from Bruker Biospin for critical discussion.

REFERENCES

(1) Altenbach, C., Kusnetzow, A. K., Ernst, O. P., Hofmann, K. P., and Hubbell, W. L. (2008) High-resolution distance mapping in rhodopsin reveals the pattern of helix movement due to activation. *Proc. Natl. Acad. Sci. U.S.A. 105*, 7439–7444.

(2) Kim, M., Xu, Q., Murray, D., and Cafiso, D. S. (2008) Solutes alter the conformation of the ligand binding loops in outer membrane transporters. *Biochemistry 47*, 670–679.

(3) Galiano, L., Ding, F., Veloro, A. M., Blackburn, M. E., Simmerling, C., and Fanucci, G. E. (2009) Drug Pressure Selected Mutations in HIV-1 Protease Alter Flap Conformations. *J. Am. Chem. Soc. 131*, 430–431.

(4) Pannier, M., Veit, S., Godt, A., Jeschke, G., and Spiess, H. W. (2000) Dead-time free measurement of dipole-dipole interactions between electron spins. *J. Magn. Reson. 142*, 331–340.

(5) Jeschke, G., Pannier, M., and Spiess, H. W. (2000) Distance Measurements in Biological Systems by EPR. In Biological Magnetic Resonance , pp 493−512, Plenum Press, New York.

(6) Bode, B. E., Margraf, D., Plackmeyer, J., Durner, G., Prisner, T. F., and Schiemann, O. (2007) Counting the monomers in nanometer-sized oligomers by pulsed electron−electron double resonance. *J. Am. Chem. Soc. 129*, 6736–6745.

(7) Pornsuwan, S., Bird, G., Schafmeister, C. E., and Saxena, S. (2006) Flexibility and lengths of bis-peptide nanostructures by electron spin resonance. *J. Am. Chem. Soc. 128*, 3876–3877.

(8) Hanson, S. M., Dawson, E. S., Francis, D. J., Van Eps, N., Klug, C. S., Hubbell, W. L., Meiler, J., and Gurevich, V. V. (2008) A model for the solution structure of the rod arrestin tetramer. *Structure 16*, 924–934.

(9) Milov, A. D., Tsvetkov, Y. D., Formaggio, F., Crisma, M., Toniolo, C., and Raap, J. (2000) Self-assembling properties of membrane-modifying peptides studied by PELDOR and CW-ESR spectroscopies. *J. Am. Chem. Soc. 122*, 3843–3848.

(10) Zhou, Z., DeSensi, S. C., Stein, R. A., Brandon, S., Song, L., Cobb, C. E., Hustedt, E. J., and Beth, A. H. (2007) Structure of the cytoplasmic domain of erythrocyte band 3 hereditary spherocytosis variant P327R: Band 3 Tuscaloosa. *Biochemistry 46*, 10248–10257.

(11) Sen, K. I., Logan, T. M., and Fajer, P. G. (2007) Protein dynamics and monomer-monomer interactions in AntR activation by electron paramagnetic resonance and double electron-electron resonance. *Biochemistry 46*, 11639–11649.

(12) McHaourab, H. S., Mishra, S., Koteiche, H. A., and Amadi, S. H. (2008) Role of sequence bias in the topology of the multidrug transporter EmrE. *Biochemistry 47*, 7980–7982.

(13) Ellenberger, T. E., Brandl, C. J., Struhl, K., and Harrison, S. C. (1992) The GCN4 Basic Region Leucine Zipper Binds DNA as a Dimer of Uninterrupted α-Helices: Crystal Structure of the Protein-DNA Complex. *Cell 71*, 1223–1237.

(14) Columbus, L., and Hubbell, W. L. (2004) Mapping backbone dynamics in solution with site-directed spin labeling: GCN4−58 bZip free and bound to DNA. *Biochemistry 43*, 7273–7287.

(15) Hanson, P., Anderson, D. J., Martinez, G., Millhauser, G., Formaggio, F., Crisma, M., Toniolo, C., and Vita, C. (1998) Electron spin resonance and structural analysis of water soluble, alanine-rich peptides incorporating TOAC. *Mol. Phys. 95*, 957–966.

(16) Inbaraj, J. J., Cardon, T. B., Laryukhin, M., Grosser, S. M., and Lorigan, G. A. (2006) Determining the topology of integral membrane peptides using EPR spectroscopy. *J. Am. Chem. Soc. 128*, 9549–9554.

(17) Traaseth, N. J., Verardi, R., Torgersen, K. D., Karim, C. B., Thomas, D. D., and Veglia, G. (2007) Spectroscopic validation of the pentameric structure of phospholarnban. *Proc. Natl. Acad. Sci. U.S.A. 104*, 14676–14681.

(18) Inbaraj, J. J., Laryukhin, M., and Lorigan, G. A. (2007) Determining the helical tilt angle of a transmembrane helix in mechanically aligned lipid bilayers using EPR spectroscopy. *J. Am. Chem. Soc. 129*, 7710–7711.

(19) Mayo, D. J., Inbaraj, J. J., Subbaraman, N., Grosser, S. M., Chan, C. A., and Lorigan, G. A. (2008) Comparing the structural topology of integral and peripheral membrane proteins utilizing electron paramagnetic resonance spectroscopy. *J. Am. Chem. Soc. 130*, 9656–9657.

(20) Gulla, S. V., Sharma, G., Borbat, P., Freed, J. H., Ghimire, H., Benedikt, M. R., Holt, N. L., Lorigan, G. A., Rege, K., Mavroidis, C., and Budil, D. E. (2009) Molecular-Scale Force Measurement in a Coiled-Coil Peptide Dimer by Electron Spin Resonance. *J. Am. Chem. Soc. 131*, 5374–5375.

(21) Prisner, T., Rohrer, M., and MacMillan, F. (2001) Pulsed EPR spectroscopy: Biological applications. *Annu. Rev. Phys. Chem. 52*, 279–313.

(22) Schweiger, A., and Jeschke, G. (2001) Multi-Frequency EPR. In Principles of pulse electron paramagnetic resonance , pp 489−500, Oxford University Press, New York.

(23) Jeschke, G., Chechik, V., Ionita, P., Godt, A., Zimmermann, H., Banham, J., Timmel, C. R., Hilger, D., and Jung, H. (2006) DeerAnalysis2006: A comprehensive software package for analyzing pulsed ELDOR data. *Appl. Magn. Reson. 30*, 473–498.

(24) Chiang, Y. W., Borbat, P. P., and Freed, J. H. (2005) The determination of pair distance distributions by pulsed ESR using Tikhonov regularization. *J. Magn. Reson. 172*, 279–295.

(25) Goger, M. J., McDonnell, J. M., and Cowburn, D. (2003) Using cryoprobes to decrease acquisition times of triple-resonance experiments used for protein resonance assignments. *Spectroscopy 17*, 161–167.